Sterically Hindered Fluorenyl-Substituted Poly(*p*-phenylenevinylenes) for Light-Emitting Diodes

Sang Ho Lee,[†] Bo-Bin Jang,[†] and Tetsuo Tsutsui*[,†,‡]

CREST, Japan Science and Technology Corporation (JST), Japan, and Department of Applied Science for Electronics and Materials, Graduate School of Engineering Sciences, Kyushu University, Kasuga, Fukuoka, 816-8580, Japan

Received April 12, 2001; Revised Manuscript Received November 14, 2001

ABSTRACT: A new series of processable dihexylfluorenyl-substituted poly(*p*-phenylenevinylene) derivatives (DHF−PPVs) were synthesized by dehydrohalogenation−condensation polymerization (GILCH polymerization). The polymers were characterized by NMR, FT-IR, and elemental analysis and were completely soluble in common organic solvents. All of the polymers demonstrated bright blue-green emission with high photoluminescence (PL) efficiencies of 68−71% in chloroform, good thermal stability with decomposition temperatures above 322 °C, and high glass transition temperatures in the range of 113−148 °C. Cyclic voltammetry studies revealed that these polymers undergo both irreversible oxidation and reduction onsets around 0.9 and −1.5 V, which are attributed to the conjugated backbone. Polymer light-emitting diodes (PLEDs), fabricated with DHF−PPVs, as the emitting layer, poly(3,4-ethylenedioxythiophene) (PEDOT) doped with poly(styrenesulfonic acid) (PSS) (PEDOT:PSS), as the hole injection/transporting layer, Ca cathodes, and indium−tin oxide (ITO) anodes, (ITO/PEDOT:PSS/DHF−PPVs/Ca), emitted blue-green emission with a maximum peak around 500 nm and a shoulder peak around 532 nm. For the poly[2-(9,9-dihexylfluorenyl)-1,4-phenylenevinylene] (DHF−PPV) device, a low turn-on voltage of 2.8 V (0.13 MV/cm), a maximum luminance of 12 000 cd/m^2 at 0.4 MV/cm, and a maximum external quantum efficiency of 0.53% were obtained. The latter was 33−37 times brighter and 1.6−2.8 times more efficient than those devices with poly[2-(7-methoxy-9,9-dihexylfluorenyl)-1,4-phenylenevinylene] (MDHF−PPV) and poly[2-(7-cyano-9,9-dihexylfluorenyl)-1,4-phenylenevinylene] (CNDHF−PPV).

Introduction

Since the first report on electroluminescence (EL) from a conjugated polymer, poly(*p*-phenylenevinylene) (PPV),[1] many studies of polymer light-emitting diodes (PLEDs) have been reported due to their potential application in full color flat panel displays.[2−4] PLEDs present many advantages such as easy fabrication with low cost, low operating voltage, color tunability, flexibility, etc.[5]

For developing practical PLEDs with a high quantum efficiency, low operating voltage, and long lifetime, the design of processable conjugated polymers with high purity and photoluminescence (PL) efficiency, good thermal and oxidation stability, and balance of charge carrier mobility is required.[4] This can be satisfied by introducing long aliphatic chains[6,7] or charge transporting materials[8−10] as pendant groups or as part of the polymer backbone or by controlling either the highest occupied molecular orbital (HOMO) or the lowest unoccupied molecular orbital (LUMO) energy level of polymer through chemical modification. For example, the functionalization of PPV through the introduction of alkoxy,[6] silyl,[7] or oxadiazole[8] units as side-chain groups on the polymer backbone or the interruption of π-conjugation along the polymer backbone in copolymers[11] provide solubility and permit tuning of the emission color as well as control of HOMO or LUMO energy levels.

Few sterically hindered polymers have been reported due to the difficulty of their synthesis. In recent years, some of conjugated polymers with phenyl,[12,13] biphenyl,[14] or 2,3-dialkoxy[15] side chains appended to the polymer backbone have exhibited excellent PL efficiencies in the solid state. Fluorene derivatives show interesting and unique chemical and physical properties because they contain a rigid planar biphenyl unit and are easily substituted at the remote C-9 position, which improves the polymer processability. Incorporating the 9,9-dialkylfluorenyl unit, where alkyl chains are out of plane to the fluorene residue, into the parent PPV backbone forms a new type of conjugated polymer, poly-[2-(9,9-dihexylfluorenyl)-1,4-phenylenevinylene] (DHF−PPV). Its geometry is nonplanar due to both a strong steric hindrance at inter-ring linking positions between the fluorene residue and the PPV backbone and intermolecular interactions due to the long side chains of the fluorene unit. In addition, the sterically hindered alkyl chains of the fluorene unit may result in an amorphous solid state of PPV, giving excellent device performance.[16] This also suppresses ordered regions within emissive layer of PLED and thus enhances the internal efficiency of the device.[17]

We have reported that sterically hindered fluorenyl-substituted PPV have excellent solubility and exhibit a high quantum efficiency from PLEDs with the configuration of ITO/PEDOT:PSS/DHF−PPV/MgAg.[18] In this study we use functionalized fluorene units (e.g., cyano- or methoxy-substituted fluorene) as pendant groups to the PPV backbone. Synthesis and characterization of the conjugated polymers, DHF−PPVs, are described, and their thermal, optical, electrochemical, and light-emitting properties are also investigated.

Experimental Section

Measurements. ^{1}H and ^{13}C NMR spectra were recorded on a JEOL JNM-LA 400 spectrometer (400 MHz) or JEOL

† CREST/JST.
‡ Kyushu University.
* To whom correspondence should be addressed. e-mail: tsuigz@mbox.nc.kyushu-u.ac.jp.

10.1021/ma010643e CCC: $22.00
Published on Web 01/17/2002

JNM-LA 600 spectrometer (600 MHz) with chloroform-*d*, dichloromethane-d_2, or DMSO-d_6 as solvents and tetramethylsilane (TMS) as the internal standard. Mass spectra were obtained with a JEOL JMS-70 spectrometer with FAB (fast-atom bombardment) system. FT-IR spectra were recorded on a BIO-RAD FTS 6000 spectrometer. UV−vis and fluorescence spectra were obtained on a Hitachi 330 spectrophotometer and on an Edinburgh Instruments FL/FS900 spectrophotometer, respectively. Thermogravimetric analysis (TGA) was conducted on a Seiko Instruments SSC 5200 TG/DTA 320 system under a heating rate of 20 °C/min and nitrogen flow rate of 80 mL/min. Differential scanning calorimetry (DSC) was run on a Seiko Instruments SII DSC 22 system. Elemental analyses were performed by Analytical Center, Kyushu University for C, H, and N determination. Cyclic voltammetry was performed on an ALS electrochemical analyzer model 660 with a three-electrode cell in a solution of Bu_4NClO_4 (0.1 M) in acetonitrile at a scan rate of 10 mV/s. Polymer films were prepared from glass coated with indium−tin oxide (ITO) by spin-coating the corresponding toluene solutions and then dried under reduced pressure. A Pt mesh was used as the counter electrode, and a Ag/AgCl (0.1 M in acetonitrile) electrode was used as the reference electrode. Prior to each series of measurements, the cell was deoxygenated with argon. Gel permeation chromatography (GPC) analysis was conducted on a Waters 515 HPLC system equipped with Waters 2487 dual λ absorbance detector and a Shodex GPC K-804 column, using polystyrene as standard and chloroform as eluent.

LED Device Fabrication and Characterization. Double-layer PLED devices were fabricated on glass substrates coated with ITO. The substrate was cleaned by a general procedure, which included sonication in detergent followed by repeated rinsing in deionized water, acetone, and ethanol, and, prior to use, placed in hot ethanol for 10 min and treated with an oxygen plasma. Conducting polymer dispersion of poly(3,4-ethylenedioxythiophene) (PEDOT) doped with poly(styrenesulfonic acid) (PSS) (PEDOT:PSS, Baytron P) was obtained from Bayer Corp. The hole injection layer of PEDOT:PSS was prepared from a water dispersion and baked at 170 °C for 20 min under argon atmosphere with the thickness of 50 nm. The emitting layers of the polymers (DHF−PPV, MDHF−PPV, and CNDHF−PPV) were spin-coated from a toluene solution onto the hole injection layer. Finally, a Ca cathode was vacuum-deposited onto the polymer layers at a pressure below 1×10^{-6} Torr. The emitting areas of the EL devices were 2×2 mm^2. EL spectra of the devices were measured by connecting a Hamamatsu PMA-11 spectrophotometer to a programmable Keithley 238 electrometer. Luminance−current density−voltage ($L-I-V$) curves were recorded with a programmable Keithley 238 electrometer and MINOLTA LS-110 colorimeter in a nitrogen atmosphere.

Materials. Tetrahydrofuran was distilled over sodium/benzophenone, 1,4-dioxane was distilled over sodium, *N*,*N*-dimethylformamide was vacuum-distilled over CaH_2, and toluene was distilled over P_2O_5. All other reagents were analytical grade quality, purchased commercially, and used without any further purification. 2-Bromo-9,9-dihexylfluorene (**1**), 2-(4,4,5,5-tetramethyl-1,3,2-dioxaborolan-2-yl)-9,9-dihexylfluorene (**2**), and 2,7-dibromo-9,9-dihexylfluorene (**10**) were prepared according to literature procedures.[19]

Diethyl 2-Bromoterephthalate (3). 2-Bromoterephthalic acid (20 g, 0.08 mol) was dissolved in 10 mL of thionyl chloride with catalytic amounts of DMF and warmed at 60 °C for 7 h. The excess thionyl chloride was removed under reduced pressure. The resulting pale yellow oil was added to 300 mL of absolute ethanol in an ice bath and stirred for 2 h at room temperature. The solvent was removed by rotary evaporation, and the crude 2-bromodiethyl terephthalate was purified by column chromatography (silica gel, hexane/ethyl acetate = 10/1) to afford a pale yellow oil (24 g) quantitatively.

2-(9,9-Dihexylfluorenyl)diethyl Terephthalate (4). To **2** (11.92 g, 26 mmol) in toluene (260 mL) and aqueous Na_2CO_3 (120 mL, 2 M) was added **3** (10.13 g, 34 mmol). After the solution was degassed with nitrogen for 20 min, tetrakis(triphenylphosphine)palladium(0) (0.6 g, 0.5 mmol) was added. The reaction mixture was refluxed with vigorous stirring under nitrogen for 24 h. After the reaction was complete, the mixture was diluted with ethyl acetate and water. The organic phase was separated and washed with brine and dried over $MgSO_4$. The crude product was purified by column chromatography (silica gel, hexane) to give 8.1 g (56.3%) of **4** as a colorless oil. ^{1}H NMR ($CDCl_3$): δ 0.50−0.70 (m, 10H), 0.90−1.10 (m, 15H), 1.30 (t, J = 8 Hz, 3H), 1.90 (t, J = 7.5 Hz, 4H), 4.00 (q, J = 7.2 Hz, 2H), 4.32 (q, J = 7.3 Hz, 2H), 7.25 (m, 4H), 7.65 (d, J = 8.2 Hz, 2H), 7.77 (d, J = 8.2 Hz, 1H), 8.00 (m, 3H).

2-(9,9-Dihexylfluorenyl)-1,4-dihydroxymethylbenzene (5). 4 (5.6 g, 0.01 mol) in 70 mL of dry THF was added dropwise with stirring to a suspension of $LiAlH_4$ (1 g, 26.3 mmol) in 100 mL of dry THF over 30 min at 0 °C. The mixture was stirred at room temperature for 30 min and further refluxed for 5 h. It was then cooled in an ice bath, and 50 mL of water was added dropwise to the suspension over 20 min. An additional 50 mL of 2 M HCl was added to destroy the remaining $LiAlH_4$. The organic layer was extracted with ethyl acetate, washed with brine, and dried over $MgSO_4$. The residue was purified by column chromatography (silica gel, hexane/ethyl acetate = 2/1) to afford 4.54 g (95.6%) as **5** of a colorless oil. ^{1}H NMR ($CDCl_3$): δ 0.60−0.70 (m, 4H), 0.75 (t, J = 7.3 Hz, 6H), 1.00−1.15 (m, 12H), 1.78 (s, 2H), 1.97 (t, J = 8.5 Hz, 4H), 4.64 (s, 2H), 4.75 (s, 2H), 7.30 (m, 7H), 7.56 (d, J = 7.7 Hz, 1H), 7.72 (m, 2H).

2-(9,9-Dihexylfluorenyl)-1,4-dichloromethylbenzene (6). To **5** (2.68 g, 5.69 mmol) in 50 mL of dry toluene was added thionyl chloride (3 mL, 34.6 mmol) containing one drop of pyridine. The reaction mixture was then heated to 100 °C for 12 h. Upon cooling to room temperature, the mixture was concentrated under reduced pressure and diluted with ethyl acetate and brine. The organic layer was separated and washed with brine and then dried over $MgSO_4$. The residue was purified by column chromatography (silica gel, hexane) to afford 2.7 g (93.5%) as **6** of a colorless oil. ^{1}H NMR ($CDCl_3$): δ 0.62−0.80 (m, 10H), 1.02−1.15 (m, 12H), 2.00 (t, J = 6.5 Hz, 4H), 4.50 (s, 2H), 4.55 (s, 2H), 7.26−7.40 (m, 6H), 7.50 (m, 2H), 7.72 (m, 2H).

2-Bromo-1,4-dihydroxymethylbenzene (7). 3 (20.9 g, 0.069 mol) in 200 mL of dry THF was added dropwise with stirring to a suspension of $LiAlH_4$ (6.5 g, 0.17 mol) in 300 mL of dry THF over 30 min at 0 °C. The mixture was stirred at room temperature for 30 min and further refluxed for 6 h. It was then cooled in an ice bath, and 15 mL of water was added dropwise to the suspension over 20 min. An additional 30 mL of 2 M HCl was added to destroy the remaining $LiAlH_4$. The organic layer was extracted with ethyl acetate, washed with brine, and dried over $MgSO_4$. The crude product was recrystallized from hexane/ethyl acetate to give 11.7 g (78%) of **7** as a white solid. ^{1}H NMR (DMSO-d_6): δ 4.48 (dd, J = 5.0 Hz, 4H), 5.28 (t, J = 5.8 Hz, 1H), 5.39 (t, J = 5.6 Hz, 1H), 7.30 (d, J = 7.8 Hz, 1H), 7.46−7.50 (m, 2H).

2-Bromo-1,4-di(2-tetrahydropyranyloxymethyl)benzene (8). To **7** (4.77 g, 0.02 mol) in DMF (3 mL) and dichloromethane (50 mL) was added 2,3-dihydropyran (5.9 g, 0.07 mol) and a catalytic amount (0.79 g) of *p*-toluenesulfonic acid. The reaction mixture was stirred for 12 h at room temperature. The organic layer was washed with brine and dried over $MgSO_4$. The residue was purified by column chromatography (silica gel, hexane/ethyl acetate = 15/1) to afford 7.25 g (86.4%) of **8** as a colorless oil. ^{1}H NMR ($CDCl_3$): δ 1.50−1.90 (m, 12H), 3.50 (s, 2H), 3.86 (s, 2H), 4.43 (dd, J = 6.6 Hz, 1H), 4.53 (dd, J = 6.3 Hz, 1H), 4.65−4.81 (m, 4H), 7.30 (s, 1H), 7.45 (s, 1H), 7.54 (s, 1H).

2-(4,4,5,5-Tetramethyl-1,3,2-dioxaborolan-2-yl)-1,4-di(2-tetrahydropyranyloxymethyl)benzene (9). To a solution of **8** (9.64 g, 0.025 mol) in dry THF (200 mL) at −78 °C was added, by syringe, 18.74 mL (0.033 mol) of *n*-butyllithium (1.6 M in hexane). The mixture was stirred at −78 °C, warmed to 0 °C for 20 min, and cooled again at −78 °C for 10 min. 2-Isopropoxy-4,4,5,5-tetramethyl-1,3,2-dioxaborolane (6.98 g, 0.037 mol) was added rapidly to the solution, and the resulting mixture was slowly warmed to room temperature and stirred for 12 h. The reaction mixture was poured into water and

extracted with ethyl acetate. The organic layer was washed with brine and dried over $MgSO_4$. The residue was purified by column chromatography (silica gel, hexane/ethyl acetate = 30/1 to 15/1) to afford 5.1 g (47.2%) of **9** as a colorless oil. ^{1}H NMR ($CDCl_3$): δ 1.30 (s, 12H), 1.50−1.90 (m, 12H), 3.53 (m, 2H), 3.93 (m, 2H), 4.50 (d, J = 12 Hz, 1H), 4.69 (t, J = 3.6 Hz, 1H), 7.47 (s, 2H), 7.76 (s, 1H).

2-Bromo-7-methoxy-9,9-dihexylfluorene (11). Sodium ethoxide was prepared by adding sodium (3.9 g, 0.17 mol) into 50 mL of anhydrous ethanol under a nitrogen atmosphere. After all the sodium disappeared **10** (16.7 g, 0.034 mol) in 150 mL of dry DMF and copper iodide (7.1 g, 0.037 mol) was added to the above solution and refluxed for 7 h. The reaction mixture was poured into ice water and then extracted with ethyl acetate. The organic layer was washed with dilute HCl and brine and dried over $MgSO_4$. The resulting oil was purified by column chromatography (silica gel, hexane) to give 7.84 g (52.1%) of **11** as a colorless oil. ^{1}H NMR ($CDCl_3$): δ 0.50−0.65 (m, 4H), 0.75 (t, J = 7.3 Hz, 6H), 1.00−1.15 (m, 12H), 1.90 (t, J = 7.6 Hz, 4H), 3.87 (s, 3H), 6.85 (m, 2H), 7.40 (m, 3H), 7.55 (d, J = 8 Hz, 1H).

2-Bromo-7-cyano-9,9-dihexylfluorene (12). A mixture of **10** (20 g, 0.04 mol) and copper cyanide (2.7 g, 0.03 mol) in 300 mL of dry DMF was refluxed for 10 h. The solvent was concentrated under the reduced pressure. To the resulting dark brown mixture was added ethyl acetate and brine. The organic phase was separated and extracted with brine and dried over $MgSO_4$. The crude product was purified by column chromatography (silica gel, hexane/ethyl acetate = 50/1) to give 6.36 g (35.7%) of **12** as a yellow solid. ^{1}H NMR ($CDCl_3$): δ 0.50−0.65 (m, 4H), 0.75 (t, J = 7 Hz, 6H), 0.95−1.15 (m, 12H), 1.97 (t, J = 7 Hz, 4H), 7.50 (t, J = 8 Hz, 2H), 7.62 (t, J = 11.5 Hz, 3H), 7.73 (d, J = 7 Hz, 1H).

2-(7-Methoxy-9,9-dihexylfluorenyl)-1,4-di(2-tetrahydropyranyloxymethyl)benzene (13). 13 was synthesized through the same condition of **4**. Colorless oil was obtained in 70% yield. ^{1}H NMR ($CDCl_3$): δ 0.60−0.70 (m, 4H), 0.75 (t, J = 7.3 Hz, 6H), 1.00−1.15 (m, 12H), 1.50−1.80 (m, 12H), 1.90 (m, 4H), 3.46 (t, J = 6.1 Hz, 1H), 3.55 (t, J = 6.1 Hz, 1H), 3.88 (s, 3H), 3.84−3.94 (m, 2H), 4.40 (d, J = 11.5 Hz, 1H), 4.56 (d, J = 12 Hz, 1H), 4.62 (t, J = 3.4 Hz, 1H), 4.71 (s, 1H), 4.75 (dd, J = 2.7 Hz, 1H), 4.87 (d, J = 10.7 Hz, 1H), 6.90 (m, 2H), 7.35 (m, 4H), 7.60 (m, 3H).

2-(7-Cyano-9,9-dihexylfluorenyl)-1,4-di(2-tetrahydropyranyloxymethyl)benzene (14). 14 was synthesized through the same condition of **4**. Colorless oil was obtained in 75% yield. ^{1}H NMR ($CDCl_3$): δ 0.50−0.65 (m, 4H), 0.78 (t, J = 6.8 Hz, 6H), 1.00−1.15 (m, 12H), 1.50−1.90 (m, 12H), 2.00 (t, J = 8 Hz, 4H), 3.46 (t, J = 6.1 Hz, 1H), 3.55 (t, J = 6.1 Hz, 1H), 3.85 (t, J = 8.8 Hz, 1H), 3.95 (t, J = 8.8 Hz, 1H), 4.40 (d, J = 11.5 Hz, 1H), 4.56 (d, J = 12 Hz, 1H), 4.63 (t, J = 3.2 Hz, 1H), 4.71 (d, J = 11.5 Hz, 1H), 4.76 (t, J = 3.7 Hz, 1H), 4.87 (d, J = 12.2 Hz, 1H), 7.36−7.47 (m, 4H), 7.60−7.69 (m, 3H), 7.78 (m, 2H).

2-(7-Methoxy-9,9-dihexylfluorenyl)-1,4-dihydroxymethylbenzene (15). A mixture of **13** (3.3 g, 4.99 mmol) and *p*-toluenesulfonic acid (0.19 g, 1.0 mmol) in 70 mL of ethanol was stirred for 5 h at room temperature. The organic layer was washed with brine, dried over $MgSO_4$, and then concentrated under reduced pressure. The crude product was purified by column chromatography (silica gel, hexane/ethyl acetate = 6/1) to give 2.3 g (92%) of **15** as a colorless oil. ^{1}H NMR ($CDCl_3$): δ 0.60−0.70 (m, 4H), 0.75 (t, J = 7.3 Hz, 6H), 1.00−1.15 (m, 12H), 1.95 (m, 4H), 3.00 (br. s, 2H), 3.85 (s, 3H), 4.60 (s, 2H), 4.65 (s, 2H), 6.88 (m, 2H), 7.25 (m, 4H), 7.50 (d, J = 7.6 Hz, 1H), 7.6 (m, 2H).

2-(7-Cyano-9,9-dihexylfluorenyl)-1,4-dihydroxymethylbenzene (16). 16 was synthesized through the same condition of **15**. Colorless oil was obtained in 87% yield. ^{1}H NMR ($CDCl_3$): δ 0.55−0.70 (m, 4H), 0.75 (t, J = 7.3 Hz, 6H), 1.00−1.15 (m, 12H), 1.75 (br. s, 2H), 2.00 (t, J = 7.6 Hz, 4H), 4.6 (s, 2H), 4.75 (s, 2H), 7.40 (m, 4H), 7.62 (m, 3H), 7.80 (d, J = 5 Hz, 2H).

2-(7-Methoxy-9,9-dihexylfluorenyl)-1,4-dichloromethylbenzene (17). 17 was synthesized through the same condition of **6**. Colorless oil was obtained in 92% yield. ^{1}H NMR ($CDCl_3$): δ 0.50−0.70 (m, 10H), 0.92−1.05 (m, 12H), 1.80−1.95 (m, 4H), 3.75 (s, 3H), 4.40 (s, 2H), 4.47 (s, 2H), 6.78 (m, 2H), 7.20 (m, 1H), 7.30 (m, 3H), 7.42 (m, 1H), 7.54 (m, 2H). Anal. Calcd for $C_{34}H_{42}Cl_2O$: C, 75.96; H, 7.87. Found: C, 75.27; H, 7.89.

2-(7-Cyano-9,9-dihexylfluorenyl)-1,4-dichloromethylbenzene (18). 18 was synthesized under the same conditions as **6**. Colorless oil was obtained in 93% yield.^{1}H NMR ($CDCl_3$): δ 0.55−0.70 (m, 4H), 0.75 (t, J = 7.2 Hz, 6H), 1.00−1.20 (m, 12H), 2.03 (m, 4H), 4.5 (s, 2H), 4.65 (s, 2H), 7.45 (m, 3H), 7.50 (s, 1H), 7.56 (d, J = 8 Hz, 1H), 7.66 (m, 2H), 7.82 (t, J = 6.8 Hz, 2H). Anal. Calcd for $C_{34}H_{39}Cl_2N$: C, 76.68; H, 7.38; N, 2.63. Found: C, 76.67; H, 7.40; N, 2.54.

Poly[2-(9,9-dihexylfluorenyl)-1,4-phenylenevinylene](DHF−PPV). 6 (3.17 g, 6.25 mmol) was dissolved in 475 mL of dry dioxane and pursed with nitrogen for 30 min at 73 °C. To the above solution was added dropwise 15.6 mL (15.6 mmol) of potassium *tert*-butoxide (1 M in hexane) for 30 min. The additional potassium *tert*-butoxide (12.5 mL, 12.5 mmol) was added, refluxed for 3 h, and cooled slowly to 45 °C. To the reaction mixture, 5 mL of mixture solvent (dioxane/acetic acid = 1/1) was added and stirred for 30 min. The reaction mixture was then poured into 500 mL of the stirred water. The resulting yellow precipitate was collected by filtration and was washed with methanol. The polymer was purified through reprecipitation of THF and methanol (three times) and dried under vacuum oven at 35 °C to afford 2.05 g (75%) of a bright yellow fiber. ^{1}H NMR (CD_2Cl_2): δ 0.70 (br s, 10H), 0.98 (br s, 12H), 1.92 (br s, 4H), 7.00−7.80 (br m, 12H). Anal. Calcd for $(C_{33}H_{38})_n$: C, 91.24; H, 8.76. Found: C, 90.24; H, 8.76.

Poly[2-(7-methoxy-9,9-dihexylfluorenyl)-1,4-phenylenevinylene] (MDHF−PPV). MDHF−PPV was synthesized through the polymerization condition of DHF−PPV. Bright yellow fiber was obtained in 70% yield. ^{1}H NMR (CD_2Cl_2): δ 0.71 (br s, 10H), 0.99 (br s, 12H), 1.90 (br s, 4H), 3.86 (s, 3H), 6.80−7.60 (br m, 11H). Anal. Calcd for $(C_{34}H_{40}O)_n$: C, 87.93; H, 8.62. Found: C, 86.15; H, 8.69.

Poly[2-(7-cyano-9,9-dihexylfluorenyl)-1,4-phenylenevinylene] (CNDHF−PPV). 18 (1.5 g, 2.82 mmol) was dissolved in 150 mL of dry THF and pursed with nitrogen gas for 30 min at room temperature. Potassium *tert*-butoxide (10 mL, 10 mmol) was added dropwise for 30 min and stirred for 48 h at room temperature. The reaction mixture was then poured into 250 mL of the stirred water. The resulting yellow precipitate was collected by filtration and was washed with methanol. The polymer was purified through reprecipitation of THF and methanol (three times) and dried under vacuum oven at 35 °C to afford 0.66 g (51%) of a bright yellow fiber. ^{1}H NMR (CD_2Cl_2): δ 0.70 (br. s, 10H), 0.97 (br. s, 12H), 1.94 (br. s, 4H), 7.00−7.80 (br. m, 11H). Anal. Calcd for $(C_{34}H_{37}N)_n$: C, 88.89; H, 8.06; N, 3.05. Found: C, 87.61; H, 8.02; N, 2.93.

Results and Discussion

Synthesis and Characterization. The monomer syntheses are depicted in Scheme 1. The DHF−PPV monomer, 2-(9,9-dihexylfluorenyl)-1,4-dichloromethylbenzene (**6**), was synthesized in four steps from the starting material, 2-bromo-9,9-dihexylfluorene (**1**), which was converted to 2-(4,4,5,5-tetramethyl-1,3,2-dioxaborolan-2-yl)-9,9-dihexylfluorene (**2**). The arylboronic ester **2** underwent Suzuki cross-coupling with diethyl 2-bromoterephthalate (**3**) using $Pd(PPh_3)_4$ catalyst to yield fluorenyl-containing diethyl terephthalate (**4**). Reduction with lithium aluminum hydride ($LiAlH_4$) and subsequent reaction with thionyl chloride finally afforded the key monomer **6**. Another synthetic route was selected to synthesize methoxy- or cyanofluorenyl-containing 1,4-dichloromethylbenzene. Diethyl 2-bromoterephthalate (**3**) was reduced with $LiAlH_4$, protected with 2,3-dihydropyran, and then treated with 2-isopropoxy-4,4,5,5-tetramethyl-1,3,2-dioxaborolane to give aryl-

Scheme 1. Synthetic Routes to the Monomers. Reagents and Conditions[a]

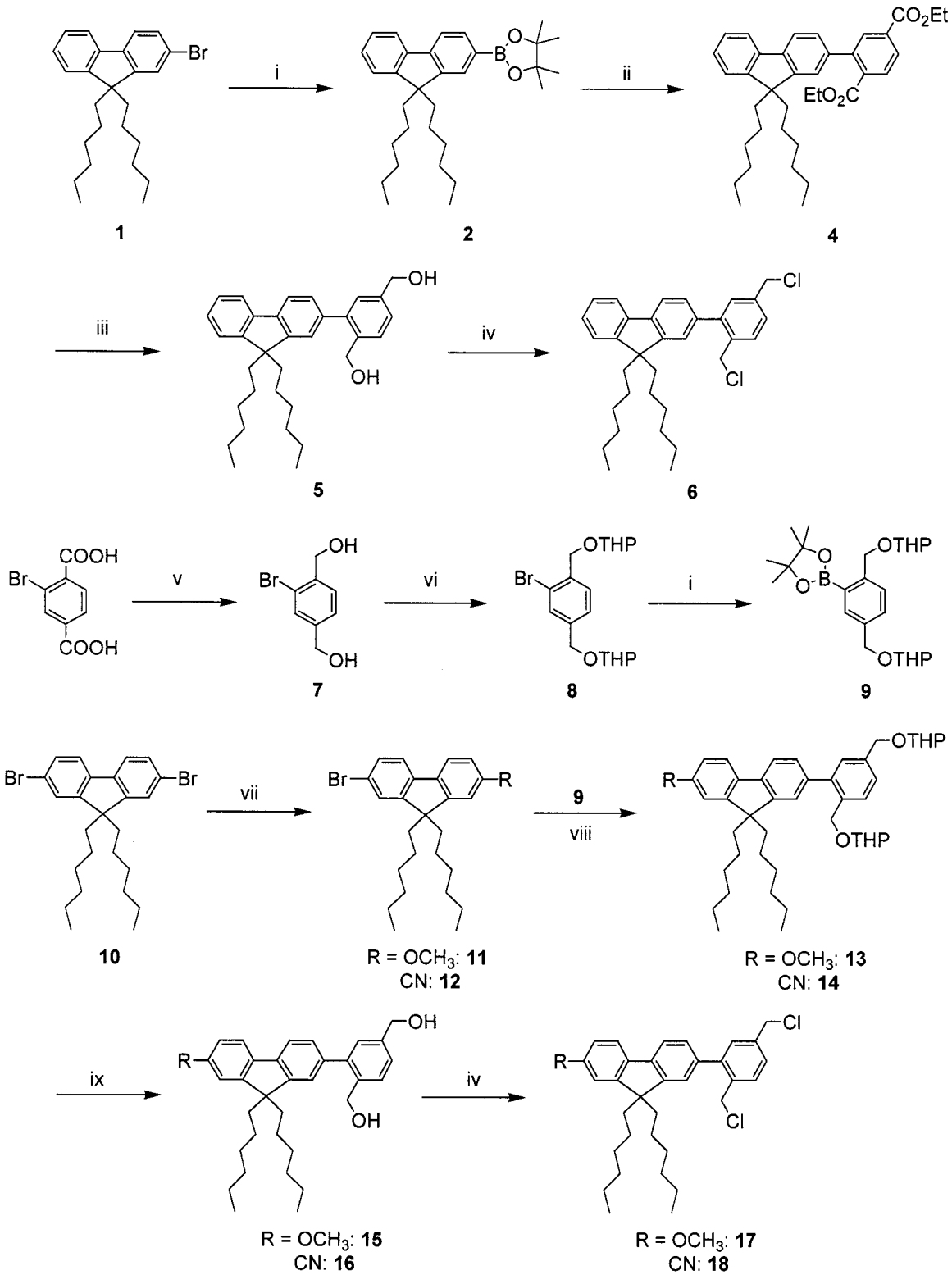

[a] (i) *n*-BuLi, 2-isopropoxy-4,4,5,5-tetramethyl-1,3,2-dioxaborolane, THF, −78 °C; (ii) **3**, $Pd(PPh_3)_4$, toluene/aqueous Na_2CO_3, reflux; (iii) $LiAlH_4$, THF, 0 °C to reflux; (iv) $SOCl_2$, toluene, 100 °C; (v) $SOCl_2$, 60 °C, EtOH, then $LiAlH_4$, THF, 0 °C to reflux; (vi) 2,3-dihydropyran, *p*-toluenesulfonic acid, DMF/CH_2Cl_2, room temperature; (vii) NaOEt, CuI, DHF, or CuCN, DMF, reflux; (viii) $Pd(PPh_3)_4$, toluene/aqueous Na_2CO_3, reflux; (ix) *p*-toluenesulfonic acid, EtOH, room temperature.

boronic ester **9**. Suzuki cross-coupling of **9** with 2-bromo-7-methoxy- or 2-bromo-7-cyano-9,9-dihexylfluorene using $Pd(PPh_3)_4$ catalyst yielded **13** or **14**, respectively. Deprotection of the tetrahydropyranyl group in **13** or **14** with *p*-toluenesulfonic acid in ethanol and subsequent treatment with thionyl chloride afforded monomers **17** or **18**, respectively. Base-induced polymerization (GILCH polymerization) of monomers **6**, **17**, or **18** with potassium *tert*-butoxide in refluxing dioxane or in THF at room temperature yielded the polymers, DHF−PPV, MDHF−PPV, and CNDHF−PPV, respectively (Scheme 2). The polymers were obtained as bright yellow fibers

Scheme 2. Synthetic Routes to Polymers, DHF−PPV, MDHF−PPV, and CNDHF−PPV

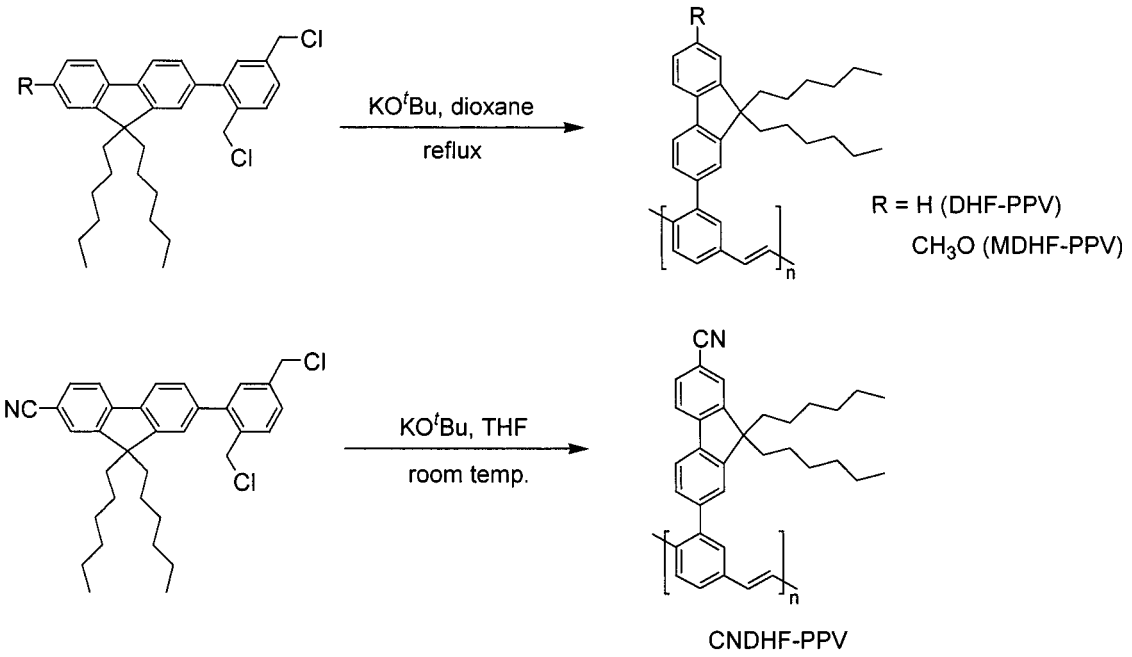

Table 1. Average Molecular Weights and Thermal Properties of DHF−PPVs

polymer	yield (%)	M_n ($\times 10^{-4}$)	M_w ($\times 10^{-4}$)	M_w/M_n	T_g (°C)	T_d (°C)
DHF−PPV	75	31.3	56.3	1.80	113	322
MDHF−PPV	70	23.8	51.9	2.18	118	331
CNDHF−PPV	51	4.2	13.2	3.13	148	345

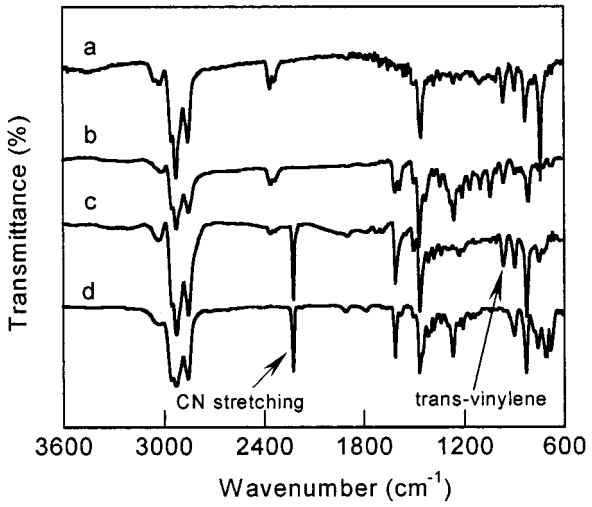

Figure 1. FT-IR spectra of (a) DHF−PPV, (b) MDHF−PPV, (c) CNDHF−PPV, and (d) monomer **18**.

after repeated precipitation with THF and methanol and readily dissolved in common organic solvents, such as chloroform, THF, toluene, and xylene.

The number-average molecular weights (M_n) and the weight-average molecular weights (M_w) of the polymers were determined to be 42 000−310 000 and 130 000−560 000 with the polydispersity index of 1.8−3.1, respectively, by gel permeation chromatography (GPC) using polystyrene as a standard (Table 1). The chemical structure of the polymers was confirmed by FT-IR, ^{1}H NMR, ^{13}C NMR, and elemental analysis. Figure 1 shows the FT-IR spectra of the polymers and the monomer **18**. The strong stretching absorption bands for C−Cl in the monomer between 660 and 800 cm^{-1} disappeared after polymerization, while a new band with strong intensity occurred at 962 cm^{-1}, which is due to the vinylic out-of-plane deformation. This result suggests that the vinylene group formed through GILCH route is in the trans configuration. The insoluble polymer, CNDHF−PPV, was obtained, when the monomer **18** was polymerized with potassium *tert*-butoxide in refluxing dioxane. This indicates that the side-reaction (e.g., the formation of cross-linked polymer) between the CN group of monomer **18** and the quinodimethane derivative formed in the first step of polymerization occurred. No observation of the sharp stretching peak of CN group at 2224 cm^{-1} in insoluble CNDHF−PPV suggests that cross-linked polymer was formed. The ^{1}H NMR spectra of the polymers and the monomer **17** exhibit the chemical shifts of alkyl side chains between 0.55 and 2.00 ppm (Figure 2). As an example, the methoxy protons (−OCH$_3$) of the monomer **17** appear at 3.75 ppm, and the methylene protons adjacent to the phenyl rings and the aromatic phenyl protons are found at 4.40 and 4.47 ppm and in the range of 6.80−7.60 ppm, respectively. As the polymerization proceeded, the methylene protons of monomer **17** around 4.40 ppm disappeared completely, and new vinylic protons appeared around 7.10 ppm.

Thermal Properties. The thermal stability of the polymers was evaluated by thermogravimetric analysis (TGA) under a nitrogen atmosphere. Figure 3 shows that the polymers exhibit good thermal stability. The polymers have onset degradation temperatures above 322 °C, and no weight loss was observed at lower temperatures. The glass transition temperatures (T_g) of the polymers were determined by differential scanning calorimetry (DSC) in a nitrogen atmosphere at a heating rate of 20 °C/min. As shown in Figure 4, all three polymers have high T_g's of 113−148 °C, which are 50−80 °C higher than that of the soluble polymer MEH−PPV (~65 °C).[20] The T_g of CNDHF−PPV is 15 °C higher than that of DHF−PPV. This can be explained by the intermolecular electrostatic interaction between the cyano groups in the fluorene units of one polymer backbone and those on adjacent chains in the bulk materials. The relatively high glass transition temper-

Table 2. Optical and Electrochemical Properties of DHF−PPVs

polymer	UV λ_{max} (nm)[a]	PL λ_{max} (nm)[a]	Φ_{PL}[b]	E_g^{op} (eV)[c]	E_g^{el} (eV)[d]	HOMO eV)[e]	LUMO (eV)[f]
DHF−PPV	428	504	0.68	2.51	2.40	−5.61	−3.21
MDHF−PPV	428	510	0.71	2.52	2.35	−5.55	−3.20
CNDHF−PPV	423	502	0.68	2.53	2.32	−5.57	−3.26

[a] Determined from thin films on the quartz plate. [b] PL efficiencies in chloroform determined relative to quinine sulfate. [c] Calculated from the absorption spectra edges. [d] Calculated from the equation E_g^{el} = LUMO − HOMO. [e] Determined from the onset of oxidative curve. [f] Determined from the onset of reductive curve.

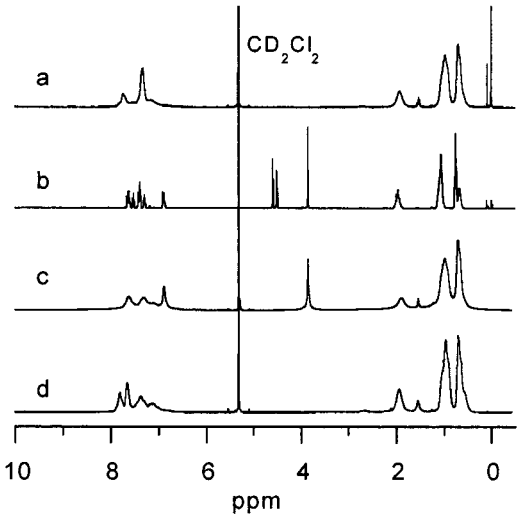

Figure 2. ^{1}H NMR spectra of (a) DHF−PPV, (b) monomer **17**, (c) MDHF−PPV, and (d) CNDHF−PPV.

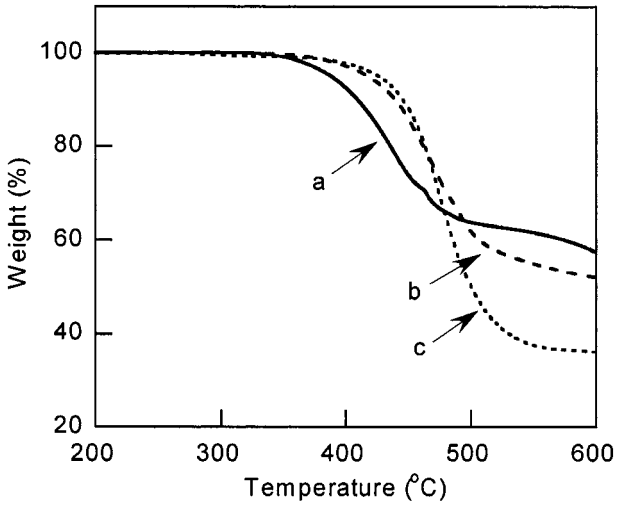

Figure 3. TGA thermograms of (a) DHF−PPV, (b) MDHF−PPV, and (c) CNDHF−PPV.

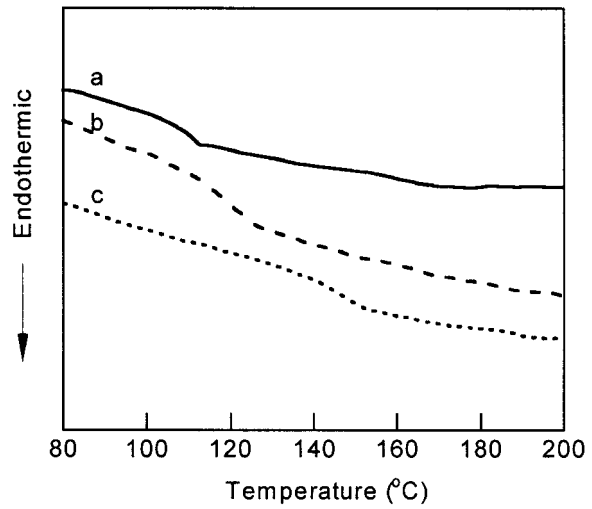

Figure 4. DSC thermograms of (a) DHF−PPV, (b) MDHF−PPV, and (c) CNDHF−PPV.

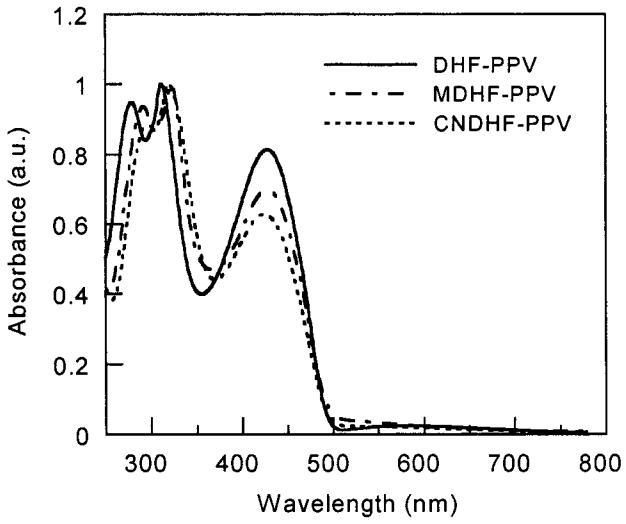

Figure 5. UV−vis spectra of (a) DHF−PPV, (b) MDHF−PPV, and (c) CNDHF−PPV films spin-coated on a quartz plate.

atures of three polymers designed as emissive materials in this study may present an advantage (e.g., improvement of the operating lifetime) for the PLED device fabrication.

Optical and Photoluminescence Properties. The UV−vis absorption of DHF−PPV, MDHF−PPV, and CNDHF−PPV as thin films is shown in Figures 5. The peak wavelengths of the spectra and the band gaps (E_g) of the polymers estimated from the absorption spectra edges are summarized in Table 2. The thin films were prepared by spin-coating on quartz plates from the polymer solutions in toluene. All three polymers exhibit very similar absorption spectra with a maximum peak of 428 nm attributed to $\pi-\pi^*$ transition of the conjugated backbones and two additional absorption peaks at 279−295 and 311−323 nm due to $\pi-\pi^*$ transition of fluorene units which are confirmed by the same two absorption peaks of the compound **1**. The absorption onset wavelengths of the polymers were the 490−494 nm, which correspond to band gaps of 2.51−2.53 eV.

The PL spectra of DHF−PPVs as thin film are shown in Figure 6. The polymer films with the broad band blue-green PL emission exhibit similar vibronic features with maximum emission peaks around 503 nm and the shoulder peaks at 530 nm, which are significantly blue-shifted compared with the two emission peaks (520 and 551 nm) of the parent polymer, poly(*p*-phenylenevinylene) (PPV). The result demonstrates that the combination of the strong steric effect[21] due to bulky groups in PPV backbone and the poor electronic effect[22] of electron-donating or -withdrawing groups in nonconjugated positions of PPV backbone gives rise to disruption

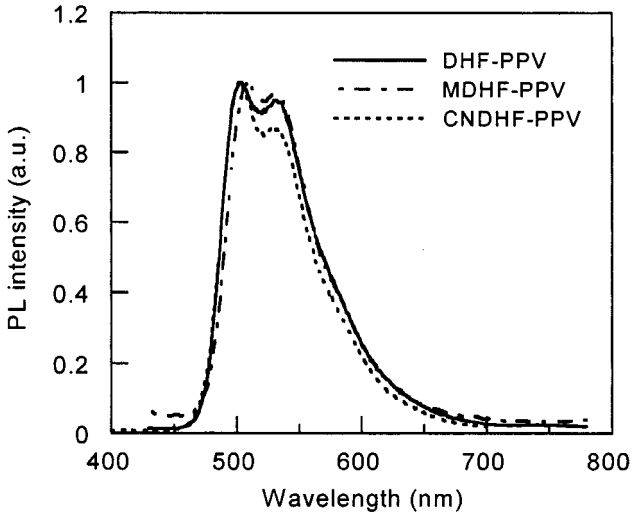

Figure 6. Photoluminescence (PL) spectra of (a) DHF−PPV, (b) MDHF−PPV, and (c) CNDHF−PPV films spin-coated on a quartz plate.

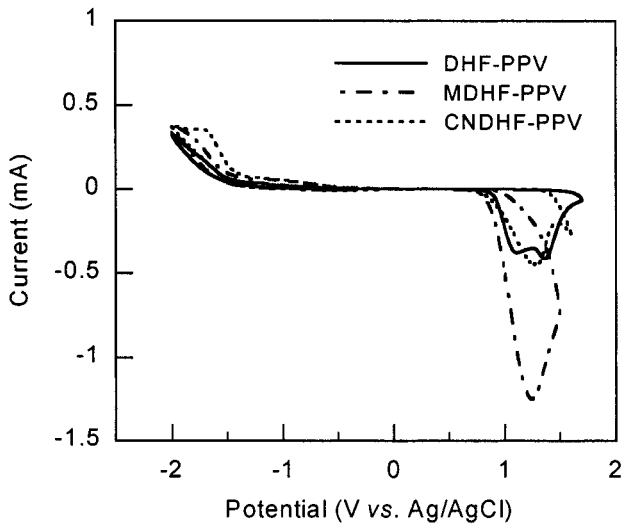

Figure 7. Cyclic voltammograms of DHF−PPVs films coated on ITO plate electrodes in acetonitrile containing 0.1 M Bu_4NClO_4. Counter electrode: platinum mesh. Reference electrode: Ag/AgCl (0.1 M in acetonitrile). Scan rate: 10 mV/s.

of the effective conjugating length of the polymer backbone. The PL efficiencies (Φ_{PL}) of the polymers in chloroform were measured by comparing to quinine sulfate (ca. 2×10^{-5} M, assuming Φ_{PL} of 0.546 at 365 nm excitation in 1 N H_2SO_4)[23] as standard. All three polymers exhibited very high PL efficiencies in chloroform in the range of 68−71%, as shown in Table 1. These PL efficiencies are comparable with those of biphenyl-substituted PPVs (73−77%), which are typical sterically hindered phenyl-substituted PPVs with maximum emission peaks of 504−520 nm in the films. The high PL efficiency of the polymers may result from the steric hindrance between fluorene units and the PPV backbone which forces the pendant fluorene unit to be twisted away from the plane of the conjugated backbone, which prevents close packing in solid state. In addition, the asymmetric bulky side group-containing DHF−PPVs will be less ordered than the symmetric side chain-containing PPV, poly(2,5-bis(2-ethylhexyloxy)-1,4-phenylenevinylene (BEH−PPV)[24] in the film state. Therefore, it is expected that PL efficiencies of DHF−PPVs thin films are less reduced.

Electrochemical Properties. Cyclic voltammetry (CV) was employed to investigate the redox behaviors of the polymers, DHF−PPVs, and to estimate the HOMO and LUMO energy levels of the polymers. The cyclic voltammograms of the polymers coated on a ITO plate from chloroform solution were performed in a three-electrode cell with a Pt counter electrode and a Ag/AgCl reference electrode. The electrolyte (0.1 M tetrabutylammonium perchlorate in acetonitrile) was purged with argon. All measurements were calibrated against an internal standard, ferrocene (Fc), which has the IP value (−4.8 eV) of the Fc/Fc^+ redox system.[25] The potential of Fc/Fc^+ was measured as 0.1 V vs Ag/AgCl in this work.

The CV curves of DHF−PPVs are shown for comparison in Figure 7. All of the polymers exhibit irreversible processes in an oxidation scan. The oxidation onsets of the polymers are 0.91, 0.85, and 0.87 V for DHF−PPV, MDHF−PPV, and CNDHF−PPV, respectively, which correspond to HOMO energy level of about 5.6 eV. The small difference of oxidation onsets for the polymers is due to the PPV backbone rather than the electronic effect of functional groups in fluorene unit. The reduction onsets of the polymers can be used for calculating LUMO energy levels and are determined to be −1.49, −1.50, and −1.45 V for DHF−PPV, MDHF−PPV, and CNDHF−PPV, respectively. As in the oxidation scan, the reduction scans of the polymers are less sensitive to the variation of substitution at the 7-position of the fluorene unit and show irreversible processes. The result demonstrates that these reduction onsets must also originate from the PPV backbone. The calculated LUMO energy levels of the polymers are about 3.2 eV, which is consistent with the results (about 3.1 eV) estimated from the HOMO and optical band gap. These values are comparable with that of cyano-substituted poly(*p*-phenylenevinylene) (CN−PPV) (3.1 eV),[26] which shows good electron transport in PLEDs.

Because of low-lying LUMO energy levels of DHF−PPVs, we believe that the operation of PLEDs fabricated using DHF−PPVs as an emitting layer and Ca (IP = 2.8 eV) as cathode would be limited by the electron mobility within the emitting layer rather than electron injection into the polymer film.

Device Characteristics. The double-layered polymer light-emitting diodes (PLEDs) with the configuration of ITO/PEDOT:PSS/DHF−PPVs/Ca were fabricated to investigate the electroluminescent properties of the new polymers, DHF−PPVs. As shown in Figure 8, all EL spectra of three DHF−PPVs show a maximum peak around 500 nm and a shoulder around 532 nm, which are very similar to the PL spectra of the corresponding polymer films. The blue-green light emission from the devices originates from the main chain of the emitting polymers. PLEDs were characterized by measuring the current density as a function of the electric field and the dependence of luminance on the electric field and by calculating the maximum external quantum efficiencies (η_{max}, %) and the turn-on voltage (MV/cm) (defined as the electric field required for a luminance of 0.1 cd/m^2). Figure 9 compares the $I-V$ curves for the double-layered diodes of ITO/PEDOT:PSS/DHF−PPVs/Ca for the three polymers. With an increasing forward bias voltage, the current in all of the devices increases, which is a typical rectifying characteristic. The EL performance of the device fabricated using a DHF−PPV emitting layer has the lowest turn-on voltage, the

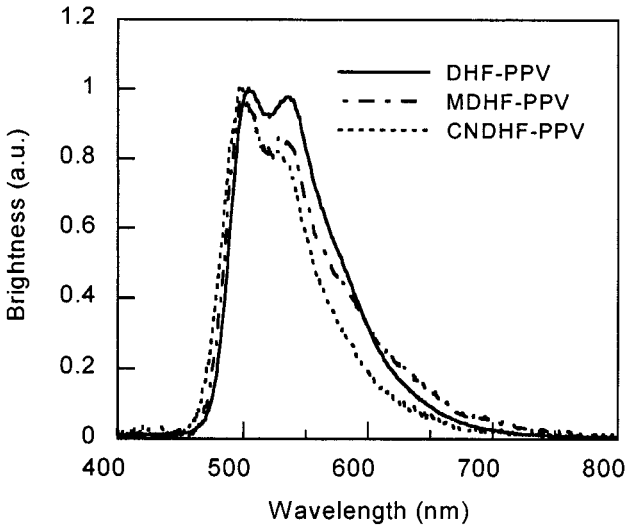

Figure 8. Electroluminescence (EL) spectra of PLEDs of (a) DHF−PPV, (b) MDHF−PPV, and (c) CNDHF−PPV with a configuration of ITO/PEDOT:PSS/DHF−PPVs/Ca.

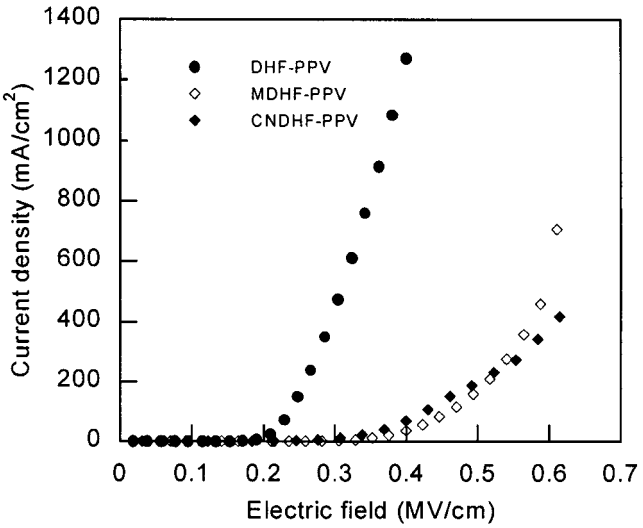

Figure 9. Current−electric field characteristics of PLEDs of (a) DHF−PPV, (b) MDHF−PPV, and (c) CNDHF−PPV with a configuration of ITO/PEDOT:PSS/DHF−PPVs/Ca.

highest maximum luminance, and the highest maximum external quantum efficiency, compared to the other two polymers. As shown by the $L-V$ curve in Figure 10, the maximum luminance of a DHF−PPV device as the emitting layer is 12 000 cd/m^2 at 0.4 MV/cm, which is 37 times higher than that of MDHF−PPV and 33 times higher than that of CNDHF−PPV at the same electric field. The turn-on voltages of DHF−PPV, MDHF−PPV, and CNDHF−PPV are 0.13, 0.21, and 0.21 MV/cm, respectively. The increase of the turn-on voltages for MDHF−PPV and CNDHF−PPV may be closely related to the carrier trapping ability of functional groups in the fluorene units. For the structure of the DHF−PPVs designed in this study, it is reasonable that the functional groups of the side fluorene units lie outside the rigid-rod polymer backbone and thus act as electron or hole carrier traps to injected charge carriers. It was found that DHF−PPV has a hole mobility of 4.3 $\times$ 10^{-4} cm^2/(V s) at an applied field of 0.25 MV/cm, which is 4 times faster than that of MDHF−PPV (1.0 $\times$ 10^{-4} cm^2/(V s)) and 3 orders faster than that of CNDHF−PPV (4.0 $\times$ 10^{-7} cm^2/(V s)) at the same applied field.[27] It means that the strong electron-withdrawing

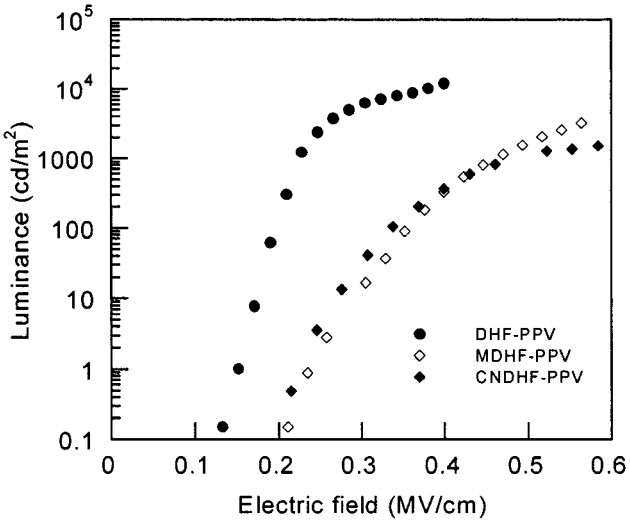

Figure 10. Luminance−electric field characteristics of PLEDs of (a) DHF−PPV, (b) MDHF−PPV, and (c) CNDHF−PPV with a configuration of ITO/PEDOT:PSS/DHF−PPVs/Ca.

CN groups in CNDHF−PPV act as deep traps of hole carriers. Furthermore, the functional groups of the side fluorene units may give rise to unbalanced charge transport in addition to the carrier trapping of injected charged carriers. Comparison of the performance of the device of DHF−PPV with those of MDHF−PPV and CNDHF−PPV shows that maximum external quantum efficiency (0.53%) of DHF−PPV is higher by a factor of 1.6 (MDHF−PPV, 0.33%) and 2.8 (CNDHF−PPV, 0.19%).

Conclusions

A new series of processable polymers with fluorene groups appended to a PPV backbone were synthesized using the dehydrohalogenation−condensation polymerization (GILCH polymerization). These polymers have quite good thermal stability with decomposition starting above 322 °C together with high glass transition temperatures in the range of 113−148 °C. The double-layer polymer light-emitting diodes (PLEDs) of dihexylfluorenyl-substituted poly(*p*-phenylenevinylene) derivatives (DHF−PPVs) emit bright blue-green light with a maximum peak around 500 nm and a shoulder peak around 532 nm. DHF−PPV devices reveal both a lower turn-on voltage (2.8 V, 0.13 MV/cm) and a greatly enhanced external quantum efficiency (0.53%) when compared to that of MDHF−PPV and CNDHF−PPV devices.

Acknowledgment. This work has been supported by the Core Research for Evolutional Science and Technology, Japan Science and Technology Corporation (CREST/JST). S.H.L. thanks Mr. Toshikazu Nakamura for his help in the CV measurement.

References and Notes

(1) Burroughes, J. H.; Bradley, D. D. C.; Brown, A. R.; Marks, R. N.; MacKay, K.; Friend, R. H.; Burn, P. L.; Holmes, A. B. *Nature (London)* **1990**, *347*, 539.
(2) Kraft, A.; Grimsdale, A. C.; Holmes, A. B. *Angew. Chem., Int. Ed.* **1998**, *37*, 402.
(3) Friend, R. H.; Gymer, R. W.; Holmes, A. B.; Burroughes, J. H.; Marks, R. N.; Taliani, C.; Bradley, D. D. C.; Dos Santos, D. A.; Brédas, J. L.; Lögdlund, M.; Salaneck, W. R. *Nature (London)* **1999**, *397*, 121.
(4) (a) Kim, D. Y.; Cho, H. N.; Kim, C. Y. *Prog. Polym. Sci.* **2000**, *25*, 1089. (b) Bernius, M. T.; Inbasekaran, M.; O'Brien, J.; Wu, W. *Adv. Mater.* **2000**, *12*, 1737.

(5) Gustafsson, G.; Cao, Y.; Treacy, G. M.; Klavetter, F.; Colaneri, N.; Heeger, A. J. *Nature (London)* **1992**, *357*, 477.
(6) Burn, P. L.; Kraft, A.; Baigent, D. R.; Bradley, D. D. C.; Brown, A. R.; Friend, R. H.; Gymer, R. W.; Holmes, A. B.; Jackson, R. W. *J. Am. Chem. Soc.* **1993**, *115*, 10117.
(7) Hwang, D.-H.; Kim, S. T.; Shim, H.-K.; Holmes, A. B.; Moratti, S. C.; Friend, R. H. *Chem. Commun.* **1996**, 2241.
(8) (a) Meng, H.; Yu, W.-L.; Huang, W. *Macromolecules* **1999**, *32*, 8841. (b) Lee, Y.-Z.; Chen, X.; Chen, S.-A.; Wei, P.-K.; Fann, W.-S. *J. Am. Chem. Soc.* **2001**, *123*, 2296.
(9) Pei, Q.; Yang, Y. *Chem. Mater.* **1995**, *7*, 1568.
(10) Yu, G.; Liu, Y.; Wu, X.; Zheng, M.; Bai, F.; Zhu, D. *Appl. Phys. Lett.* **1999**, *74*, 2295.
(11) (a) Ahn, T.; Jang, M. S.; Shim, H.-K.; Hwang, D.-H.; Zyung, T. *Macromolecules* **1999**, *32*, 3279. (b) Pang, Y.; Li, J.; Hu, B.; Karasz, F. E. *Macromolecules* **1999**, *32*, 3946.
(12) Hsieh, B. R.; Yu, Y.; Forsythe, E. W.; Schaaf, G. M.; Feld, W. A. *J. Am. Chem. Soc.* **1998**, *120*, 231.
(13) (a) Spreitzer, H.; Becker, H.; Kluge, E.; Kreuder, W.; Schenk, H.; Demandt, R.; Schoo, H. *Adv. Mater.* **1998**, *10*, 1340. (b) Johansson, D. M.; Srdanov, G.; Yu, G.; Theander, M.; Inganäs, O.; Andersson, M. R. *Macromolecules* **2000**, *33*, 2525.
(14) Peng, Z.; Zhang, J.; Xu, B. *Macromolecules* **1999**, *32*, 5162.
(15) Martin, R. E.; Geneste, F.; Riehn, R.; Chuah, B. S.; Cacialli, F.; Friend, R. H.; Holmes, A. B. *Chem. Commun.* **2000**, 291.
(16) Adachi, C.; Tsutsui, T.; Saito, S. *Appl. Phys. Lett.* **1990**, *56*, 799.
(17) Conwell, E. *Trends Polym. Sci.* **1997**, *5*, 218.
(18) (a) Lee, S. H.; Jang, B.-B.; Tsutsui, T. *Proc. SPIE* **2000**, *4105*, 322. (b) Lee, S. H.; Jang, B.-B.; Tsutsui, T. *Chem. Lett.* **2000**, 1184.
(19) Lee, S. H.; Tsutsui, T. *Thin Solid Films* **2000**, *363*, 76.
(20) Kim, J. L.; Kim, J. K.; Cho, H. N.; Kim, D. Y.; Kim, C. Y.; Hong, S. I. *Macromolecules* **2000**, *33*, 5880.
(21) Chung, S.-J.; Jin, J.-I.; Lee, C.-H.; Lee, C.-E. *Adv. Mater.* **1998**, *9*, 684.
(22) Detert, H.; Sugiono, E. *Synth. Met.* **2000**, *115*, 89.
(23) Demas, J. N.; Crosby, G. A. *J. Phys. Chem.* **1971**, *75*, 991.
(24) Andersson, M. R.; Yu, G.; Heeger, A. J. *Synth. Met.* **1997**, *85*, 1275.
(25) Pommerehne, J.; Vestweber, H.; Guss, W.; Mahrt, R. F.; Bässler, H.; Porsch, M.; Daub, J. *Adv. Mater.* **1995**, *7*, 551.
(26) Cervini, R.; Li, X.-C.; Spencer, G. W. C.; Holmes, A. B.; Moratti, S. C.; Friend, R. H. *Synth. Met.* **1997**, *84*, 359.
(27) Lee, S. H.; Yasuda, T.; Tsutsui, T., unpublished results.

MA010643E